agronomy

MDPI

Article

An Air Convection Wall with a Hollow Structure in Chinese Solar Greenhouses: Thermal Performance and Effects on Microclimate

Yunfei Zhuang [1,2], Shumei Zhao [1,*], Jieyu Cheng [1], Pingzhi Wang [1], Na Lu [3], Chengwei Ma [1], Wenxin Xing [4] and Kexin Zheng [1]

[1] Key Laboratory of Agricultural Engineering in Structure and Environment, Ministry of Agriculture and Rural Affairs, College of Water Resources and Civil Engineering, China Agricultural University, Beijing 100083, China; zhuangyunfei1015@outlook.com (Y.Z.); 13301232820@cau.edu.cn (J.C.); wpz@cau.edu.cn (P.W.); macwbs@cau.edu.cn (C.M.); zkx940421@163.com (K.Z.)
[2] Graduate School of Horticulture, Chiba University, Matsudo 271-8510, Japan
[3] Center for Environment, Health and Field Sciences, Chiba University, Kashiwa 277-0882, Japan; na.lu@chiba-u.jp
[4] Beijing Zhongnong Futong Horticulture Co., Ltd., Beijing 100083, China; xingwenxin3344@163.com
* Correspondence: zhaoshum@cau.edu.cn

Abstract: A Chinese solar greenhouse (CSG) is a horticultural facility that uses solar energy to promote a growth environment for crops and provides high-efficiency thermal storage performance to meet the demand of vegetables' growth in winter. Besides being an important load-bearing structure in CSGs, the north wall is a heat sink, storing during the day in order to act as a heat source during the night. At times, the night temperature is lower than the minimum growth temperature requirement of vegetables, and the additional heating is needed. Therefore, optimizing the heat storage and release performance of the north wall in a CSG is an important approach for improving growth environment and reducing consumption of fossil fuel. This study proposes a heat storage north wall with a hollow layer on the basis of air convection, aiming to optimize the utilization of solar energy in CSGs. By the air convection effects, the hollow layer collects and stores surplus solar energy in the air during the day and transfers it to the cultivation space for heating at night. Additionally, field tests were conducted to compare the natural and forced convection strategies via airflow and heat transfer efficiency. The final effect on the indoor temperature ensured that the lowest temperatures at night were above 5 °C under both the natural and forced convection strategies during the winter in the Beijing suburbs where the average minimum temperature is below −10.8 °C during the experimental period. The hollow structure improves the utilization efficiency of solar energy in CSGs and ensures winter production efficiency in northern China.

Keywords: Chinese solar greenhouse; low temperature heating; passive heat-storage wall; thermal performance; microclimate

Citation: Zhuang, Y.; Zhao, S.; Cheng, J.; Wang, P.; Lu, N.; Ma, C.; Xing, W.; Zheng, K. An Air Convection Wall with a Hollow Structure in Chinese Solar Greenhouses: Thermal Performance and Effects on Microclimate. *Agronomy* **2022**, *12*, 520. https://doi.org/10.3390/agronomy12020520

Academic Editors: Jouke Campen and Feije de Zwart

Received: 24 December 2021
Accepted: 17 February 2022
Published: 19 February 2022

1. Introduction

A Chinese solar greenhouse (CSG) is a horticultural facility that uses solar energy to promote a growth environment for crops and provides high-efficiency thermal storage performance to meet the demand of vegetables' growth in winter [1]. By absorbing short wave radiation, storing heat and reducing convective and longwave radiative heat loss, a CSG with a closed structure maintains a suitable environment for the intensive production of various crops [2,3]. The main structures of CSGs include a steel frame, a north wall (north side), two sidewalls (east side and west side), a single-layer plastic cover (south roof), and a thermal insulation blanket [4]. Besides being an important load-bearing structure in CSGs, the north wall is a heat sink while storing during the day in order to act as a heat

source during the night [5,6]. Six shapes of greenhouses in Iran were compared from the perspective of energy demand, showing that an east–west oriented single-span greenhouse with a north wall was the optimum option. Moreover, insulation of the north wall reduced the heat losses substantially. [7]. Therefore, the structural innovation of the north wall and its effects on heat storage and release have been a hot spot on the issue of improving the thermal performance of CSGs.

The thermal preservation and insulation performance of CSGs sustains a significant higher temperature inside the facility than outside in the winter, with a temperature difference of 15 to 40 °C [8,9]. However, cold damage will still be caused by low temperature at night in winter [10]. Especially in cold northern China, additional heating is necessary for crop growth, but this increases the fossil fuel consumption and causes environmental pollution. In addition, the temperature of CSGs in sunny winter afternoons tends to rise to 40 °C, which necessitates ventilation and cooling [11,12]. Ventilation causes heat loss during the day, which is even more detrimental for greenhouses equipped with CO_2 enrichment devices. Therefore, collecting the surplus solar energy received by CSGs during the day and using it for indoor space low temperature heating at night is an effective way to improve the crop growth comfort and reduce fossil fuel consumption [13].

Greenhouses need separate passive [14] or active [15] heating systems to maintain a suitable microenvironment during cold winters [16]. Passive heating in CSGs relies heavily on the north wall [17]. The structure and materials of the north wall were studied based on passive heating theory [18]. Many studies focus on the combination of building materials for walls [19,20], the application of specialty materials [21,22] and the development of phase change materials [23–27]. These studies provide a variety of options for the north wall of CSGs, and contribute to the issue of the environment balance of CSGs. However, the stability of the material combination, the range of applications, and the safety and cost of phase change materials require further analysis and evaluation. More importantly, merely changing the material and composition of the wall cannot increase the heat storage area of the north wall [28], and expansion of the wall area involved in heat storage is beneficial to improve the efficiency of solar energy utilization. On the other hand, some studies have revealed that the depth of the north wall involved in heat storage is limited, and blindly increasing the wall thickness cannot improve the heat storage and preservation performance [29,30]. A way to improve the heat storage of the north wall is to mobilize the parts of the north wall that could not participate in heat storage. Therefore, it is crucial to expand the surface area involved in the heat transfer between the indoor air of CSGs and the north wall so that more volume of the north wall could be used for heat storage and release.

In order to expand the heat transfer surface area and increase the heat storage volume of the north wall in CSGs for optimizing the utilization of solar energy and improve the thermal comfort of the microenvironment in winter, we proposed a design of heat storage north wall with a hollow layer on the basis of air convection [31]. There is a hollow structure within the north wall, and the internal space of the hollow layer exchanges heat with the cultivation space. By the air convection effects, the hollow layer collects and stores surplus solar energy in the air during the day and transfers it to the cultivation space for heating at night. Additionally, circulating fans are added to the wall structure to generate a stable airflow to enhance the heat exchange effect. Field experiments were conducted during the winter in the Tongzhou District, Beijing (39.9° N 116.6° E, elevation 8.2–27.6 m) to analyze the thermal performance under two air convection strategies.

2. Materials and Methods

2.1. Air Convection Heat Storage North Wall Design Criteria and Air Convection Mechanism

The innovation of this design is to connect the hollow layer of the north wall to the indoor environment. The air density difference between the cultivation space and the hollow layer can drive the heat exchange between the two spaces to increase the north wall's heat storage during the day and the heat release at night. In this design, the availability

of local construction materials and the simplicity of construction are fully considered to lower the construction cost and facilitate the promotion of this wall design. Therefore, concrete hollow blocks, which are commonly used in the construction of CSGs in Beijing, are selected as the construction material for the north wall. Since the size of the concrete hollow block is 200 mm × 200 mm × 400 mm, the inner layer is designed to be 400 mm and the outer layer is designed to be 200 mm according to the placement. The hollow layer is designed to be 600 mm because of reducing the air flow resistance and ensuring the load-bearing safety of the north wall.

Figure 1 shows the structure of the air convection heat storage north wall in this study. The wall was composed of an 'Inner layer' (concrete hollow block filled with mortar, 400 mm thick), 'Hollow layer' (600 mm thick), 'Outer layer' (concrete hollow blocks filled with mortar, 200 mm thick), and 'Insulation layer' (extruded board, 70 mm thick) from inside to outside (Figure 1a). Reinforcement structures in the hollow layer were arranged at equal intervals to ensure the strength of the wall. Two rows of vents (size: 140 mm × 140 mm, 264 per row) from east to west were arranged on the upper and lower parts of the inner layer, and the height difference between the upper and lower rows of vents was 2 m (Figure 1b).

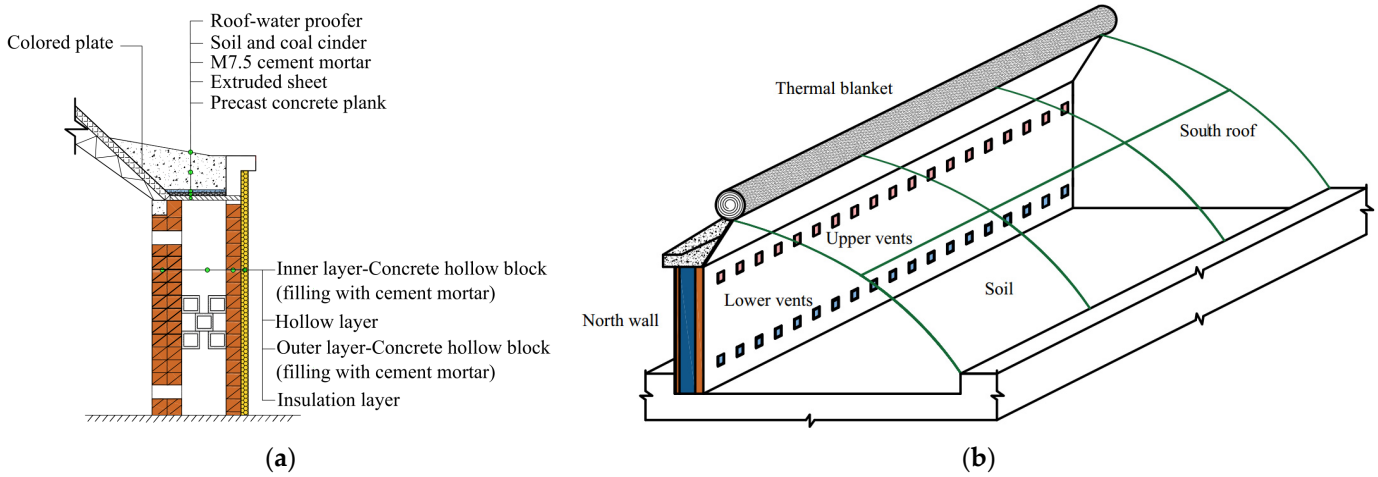

Figure 1. Structure of the air convection heat storage north wall: (**a**) Schematic of the air convection north wall with a hollow structure; and (**b**) schematic of the indoor surface with vents.

Natural air convection is formed by the air density difference between the hollow layer of the north wall and the cultivation space. As the temperature in the CSG rises rapidly during the day, the temperature difference between the inside and outside of the hollow layer gradually increases. The hot air in the CSG rises due to low density, and the cold air in the hollow layer sinks due to high density. The hot air enters the hollow layer through the upper vents, while the cold air enters the CSG through the lower vents (Figure 2a). Natural convection brings the hot air into the hollow layer and stores the heat inside the wall through heat convection. At night, a circulation airflow in the opposite direction is formed, and the airflow brings the stored heat during the day back to the CSG for nighttime heating (Figure 2b).

On this basis, in order to assist in regulating the circulating air flow, fans (130 mm × 130 mm, rated power 4.3 W) are installed in the upper vents, and forced convection is generated by the operation of the fans. In this process, the fans force the air from the lower vents into the hollow layer and the circulation direction is from bottom to top in the hollow layer. Different from natural convection, forced convection is mono-directional during fans operation, circulating in the opposite direction to natural convection during the day and in the same direction as natural convection during the night.

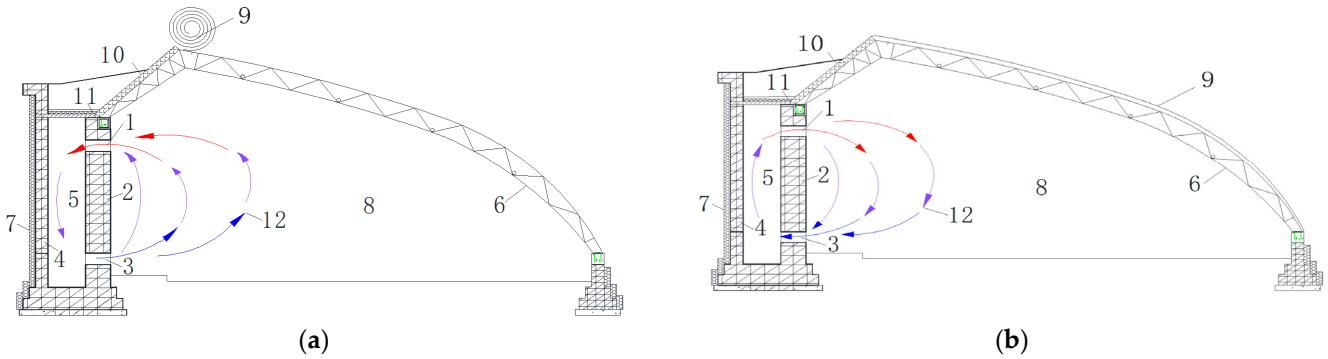

Figure 2. Circulation direction of natural convection: (**a**) circulation direction during the day; and (**b**) circulation direction at night. (1) Upper vent, (2) inner layer of north wall, (3) lower vents, (4) outer layer of north wall, (5) hollow layer, (6) gable south roof frame, (7) insulation layer, (8) cultivation space, (9) thermal blanket, (10) north rear roof, (11) insulation layer, and (12) direction of airflow (Red indicates hot air and blue indicates cold air).

2.2. Experiment Setup

The experimental CSG (Figure 3) applied a north wall with a hollow structure and the azimuth angle is 5° southwest. The indoor floor area was 480 m^2 (8 m wide and 60 m long) and the height of the north wall (gray surface) was 2.6 m with an air convection hollow structure. The front roof and the back roof were steel semiarch welded truss structures. A 0.08-mm-thick polyolefin film (transmittance is 90%) was used as the covering material for the south roof, and a cotton thermal blanket was used to reduce thermal loss through the south roof at night. In the experimental CSG, the thermal blanket was rolled up at 08:20 and dropped at 17:00 during the experimental period. During the experiment, there was no plant production.

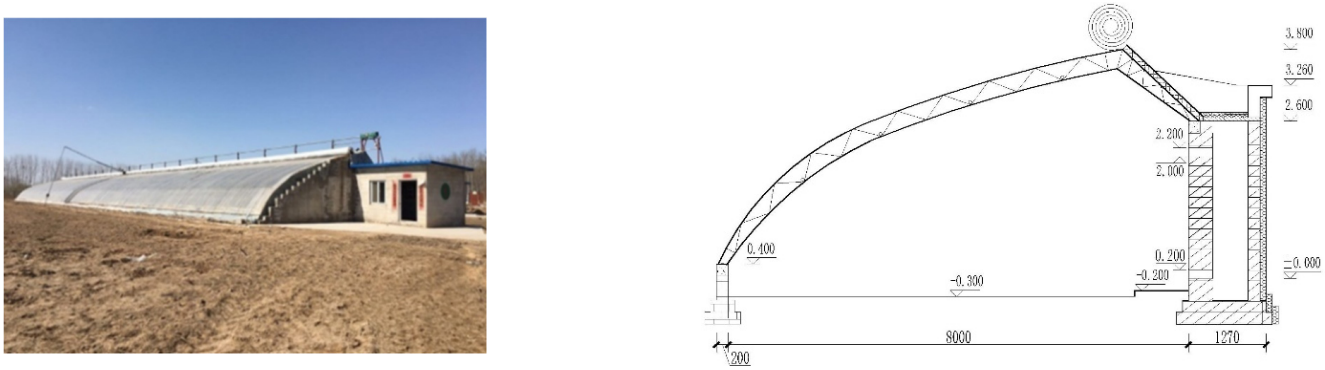

Figure 3. Field and structure of the experimental Chinese solar greenhouse. Note: The units of height and span are meter (m) and millimeter (mm), respectively.

2.3. Experiment Design

In this study, the experimental CSG was divided into two areas in the east–west direction (the test and control areas). The two areas were separated by a double-layer plastic film. Additionally, double-layer plastic films were used for partitions near the east and west sidewalls to minimize boundary intrusion. The field tests were conducted in the experimental CSG from 20 December 2017 to 6 March 2018 during the winter. Two comparative experiments were designed: (1) comparison of the wall with natural internal convection and the wall with blocked internal convection (S1); and (2) comparison of the wall with natural internal convection and the wall with forced internal convection (S2). Table 1 shows the experiment design.

Table 1. Experiment design of S1 and S2.

Comparative Experiments	Experimental CSG			Period
	Test Area (Western Half)	Control Area (Eastern Half)	Boundaries	
S1	Wall with natural internal convection (NCW)	Wall with blocked internal convection (NW)	7.5 m from the eastern and western sidewalls	From 20 December 2017 to 23 January 2018
S2	Wall with forced internal convection (FCW)	Wall with natural internal convection (NCW)		From 26 January 2018 to 6 March 2018

2.4. Data Collection

Data collection was focused on the velocity of air convection, the temperature of the air and internal wall, the heat flux of the wall surface, and the enthalpy change of the vents. Figure 4 shows the measurement schemes used in the CSG to obtain these parameters. Multiple air velocity sensors monitored the air convection velocity, which the lowest measurement limit is 0.15 m s^{-1}. Air temperatures in the CSG were measured by T-type thermocouples (accuracy: ±0.5 °C). T-type thermocouples also measured the temperatures at different depths inside the wall (the temperature measurement points inside the wall were buried during its construction). The heat flux density on the wall surface was measured using several heat flux plates (HUKSEFLUX, Netherlands, accuracy: ±3% of reading). The time interval for data collection was 10 min. Figure 3 shows the measurement positions. Additionally, two pairs of vents were selected at equal intervals in the control and test areas for the testing of the dry and wet bulb temperatures in the upper and lower vents. The test was performed every two hours from 18:00 until 08:00 the next day. The dry and wet bulb temperatures in the vents were measured using an H-AMZ-ON ventilated dry and wet meter (ISUZU, Japan, accuracy: 0.1 °C).

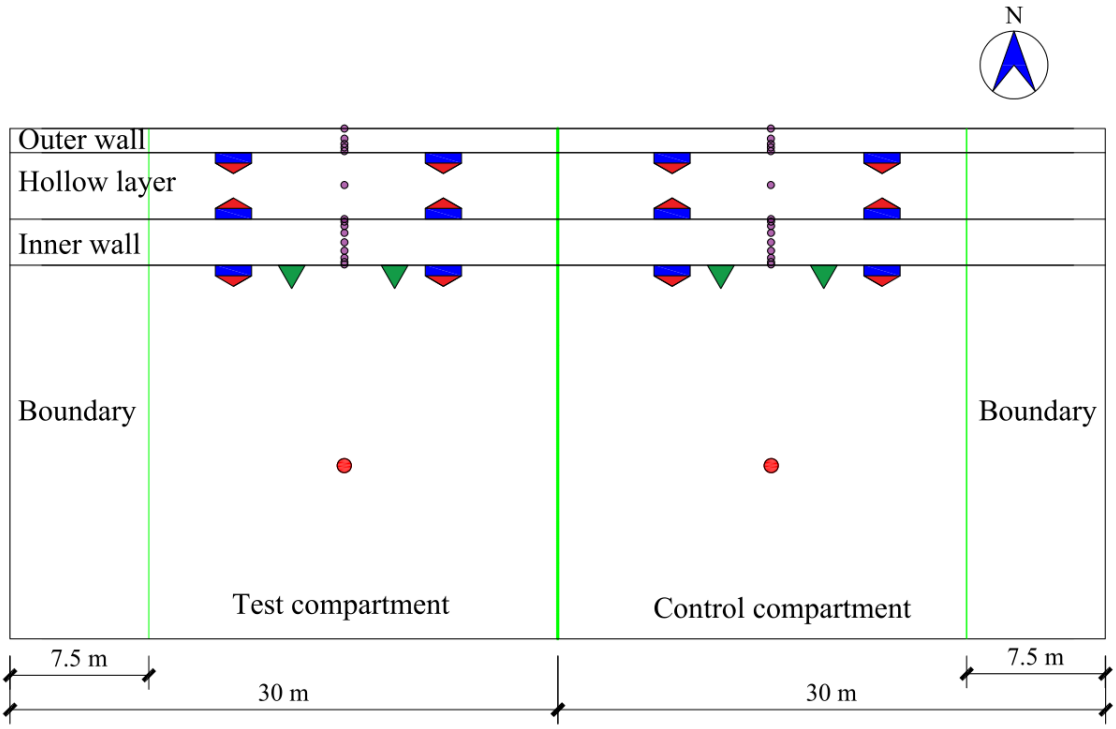

(a)

Figure 4. *Cont.*

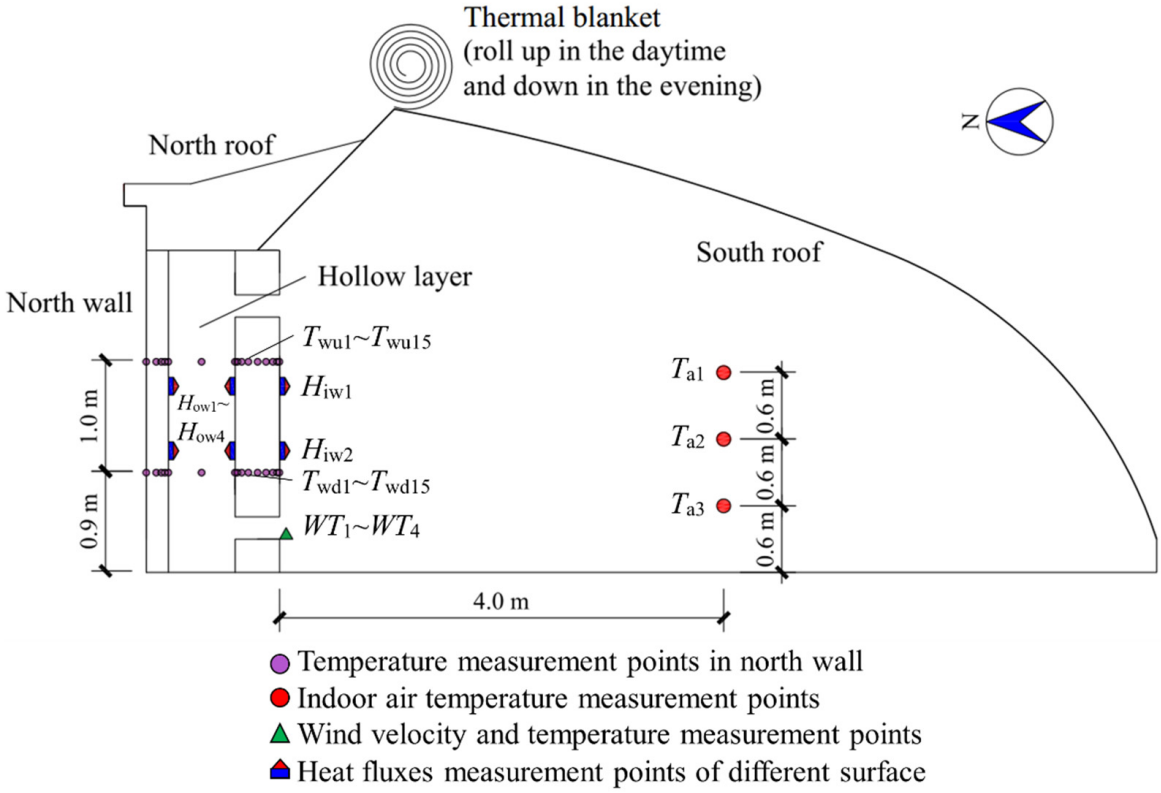

(b)

Figure 4. Schematic of the sensor locations and measuring points: (**a**) vertical view; (**b**) side view. Note: The air temperatures of the test and control compartments are averaged with T_{a1}–T_{a3}; the air velocity and temperature of the vents are averaged with WT_1–WT_4; the heat flux of the indoor wall surface is averaged with H_{iw1} and H_{iw2}; the heat fluxes of the hollow layer surfaces are averaged with H_{ow1}–H_{ow4}; and the internal temperature of the north wall is averaged with T_{wu} and T_{wd} at the same depth (e.g., the temperature at 0 mm is represented by the average of T_{wu1} *and* T_{wd1}).

2.5. Heating Performance Analysis

2.5.1. Temperature Enhancement of Wall Interior and Air

During the winter nights, the indoor temperature of CSGs is directly affected by space heating [32]. Thus, in the comparison experiments, the temperature distribution inside the wall is used to illustrate the difference in the depth of heat storage and release. Additionally, the indoor air temperature demonstrates the effects of different walls on the space heating.

2.5.2. Theoretical Calculation of Air Convection

The core of the air convection heat storage wall is where the generation of the air convection and the heat exchange occurs. Hence, the value and trend of the air convection velocity must be determined.

According to the natural ventilation theory, the theoretical airflow is calculated as follows [33]:

$$L_\alpha = k\sqrt{\frac{2gh(t_u - t_d)}{T_u}}, \quad (1)$$

$$k = \frac{1}{\sqrt{\frac{1}{\mu_1^2 F_1^2} + \frac{1}{\mu_2^2 F_2^2}}}. \quad (2)$$

where L_α is the theoretical airflow ($m^3\ s^{-1}$); k is the calculation coefficient of airflow; t_u and t_d are the air temperatures of the upper and lower vents (°C); h is the center-to-center spacing between the upper and lower vents (m); T_u is the thermodynamic temperature of the vents on the wall (K); F_1 and F_2 are the upper and lower vent areas (m^2); and μ_1 and μ_2 are the upper and lower vent airflow coefficients.

According to [33], the airflow coefficients μ_1 and μ_2 in natural ventilation are determined by the aspect ratio of the window and the opening angle. Since the upper and lower vents in this study are square and unobstructed, which can be regarded as open windows, the values of the airflow coefficients μ_1 and μ_2 are 0.65.

2.5.3. Heat Transfer Efficiency and Accumulation

The heat exchange per unit time of convective air is analyzed through the air state of the upper and lower vents. The heat exchange represents the heat loss after the hot air passes through the hollow layer. The heat is left in the hollow layer, a part of which is the sensible heat (heat exchange between hot and cold air) and the other is the latent heat (condensation occurs in the hollow layer). The hollow layer releases heat at night, and the heat is taken to cultivation space after the cold air passes through the hollow layer. The instantaneous heat exchange can be calculated as follow [34]:

$$\Phi_{i,t} = m_{air}\left(h_{U_{i,t}} - h_{L_{i.t}}\right) = \rho_{air} L_\alpha \left(h_{U_{i,t}} - h_{L_{i.t}}\right), \quad (3)$$

where $\Phi_{i,t}$ is the heat exchange of the wall at time t under convection strategy i (kW); $h_{Ui.t}$ and $h_{Li.t}$ are the specific enthalpies of the upper and lower vent air at time t under convection strategy i (kJ kg^{-1}); m_{air} is the mass flow of convective air (kg s^{-1}); and ρ_{air} is the indoor air density (kg m^{-3}).

On the basis of the heat flux inside and outside the hollow layer, cumulative heat storage and release are calculated as follows [35]:

$$\begin{aligned} Q_s &= \sum q_s \times t, \\ Q_r &= \sum q_r \times t, \end{aligned} \quad (4)$$

where Q_s is the accumulated heat of the wall during heat storage (MJ m^{-2}); Q_r is the accumulated heat of the wall during heat release (MJ m^{-2}); q_s is the heat flux density of heat storage (W m^{-2}); q_r is the heat flux density of heat release (W m^{-2}); and t is the time interval of measurement (600 s).

2.5.4. Dehumidification Potential

The convective heat exchange process of the circulating airflow in the hollow layer contains both sensible heat and latent heat changes. The latent heat change is primarily due to the process of condensation of hot air after entering the hollow layer. Hence, the wall structure has a certain dehumidification potential that can be calculated as [34]:

$$D_{i,t} = m_{air}\left(d_{U_{i,t}} - d_{L_{i.t}}\right) = \rho_{air} L_\alpha \left(d_{U_{i,t}} - d_{L_{i.t}}\right), \quad (5)$$

where $D_{i,t}$ is the dehumidification of the wall at time t under convection strategy i (g s^{-1}), and $d_{Ui.t}$ and $d_{Li.t}$ are the humidity ratios of the upper and lower vent air at time t under convection strategy i (kg kg^{-1}).

2.5.5. Coefficient of Performances (COP) for Air Convection Wall with Forced Convection

The hollow layer with forced convection is regarded as an active solar heating system, which can be evaluated by the coefficient of performance (COP). The COP is the ratio of the energy released from the active solar heating system to power consumption of both heat storage and release that can be calculated as [36]:

$$COP = \frac{Q_r}{P_e(t_s + t_r)} \quad (6)$$

where Q_r is the energy released from the active solar heating system (J); P_e is the rated power of the fans, 4.3 W; and t_s and t_r are the duration of heat storage and release (h).

3. Results and Discussion

3.1. Indoor Temperature Changes under Different Conditions

The most important effects of the wall structure on the cultivation environment of the CSG is the change in indoor day and night temperature. Figure 5a shows the changes of indoor and outdoor temperatures of the NCW and NW. The average daily temperature from January 15 to 22 was −2.5 °C, with the lowest nighttime temperature low below −10 °C on January 18 to 21. The differences between indoor and outdoor air temperatures of NCW and NW at night were 17.3 °C and 16.0 °C. Compared to NW, both of the average and minimum nighttime temperatures of NCW were 1.3 °C higher, indicating that natural convection elevated the indoor temperature levels in CSG. The role of the north wall with hollow structure in improving the thermal environment of CSGs was demonstrated.

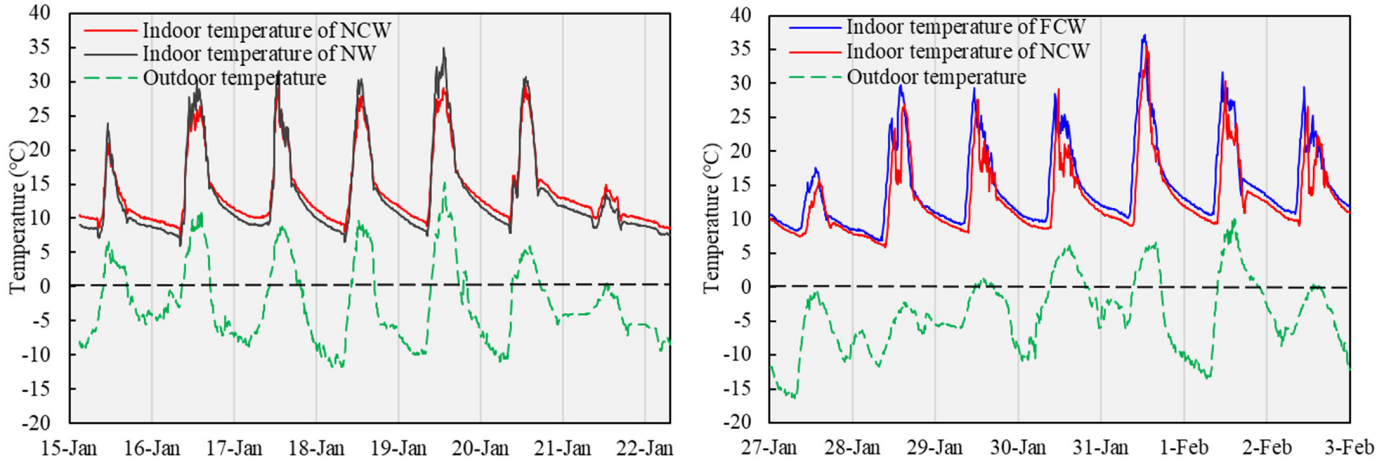

Figure 5. Comparison of indoor and outdoor temperatures under different conditions: (**a**) NCW and NW; and (**b**) NCW and FCW.

Figure 5b shows the indoor air temperature changes of the FCW, the NCW, and the outdoor air from January 27 to February 3. The average outdoor temperature during the experiment was −4.2 °C (the lowest temperature reached −16.2 °C). The indoor temperature was maintained at a relatively high temperature, and the average indoor and outdoor temperature differences of the NCW and FCW at night were 17.2 °C and 18.2 °C, respectively. Even on a cloudy day, the indoor temperature at night was kept above 5 °C with both strategies, which effectively avoided cold damage caused by low temperatures at night. The average night temperature (17: 30 to 8: 00 the next day) of the FCW was 1.0 °C higher than that of the NCW, and the average lowest temperature at night of the FCW and the NCW were 9.1 °C and 8.1 °C, respectively. The results show that the forced convection can further enhance the contribution of the north wall to raise the indoor temperature of CSG compared to a system solely based on the natural convection. The higher nighttime indoor temperature of FCW means that forced convection mobilizes more available heat from the north wall than natural convection, resulting in better efficiency of heat release.

3.2. Temperature Distribution along the Depth of the Wall

A typical sunny day (16 January 2018) was chosen as the representative day for analysis to compare the effect of the presence or absence of air convection on the temperature distribution of the wall (Figure 6a,b). The average nighttime temperature was −4.3 °C and the average daytime temperature was 6.0 °C. The highest outdoor temperature was 11.2 °C, and the lowest outdoor temperature was −7.3 °C. From the temperature distribution along the depth direction, the NCW shows several 'peaks' and 'valleys', and there are temperature fluctuations in the depth range of 600–1000 mm. It implies that there is a temperature

difference inside the walls of NCW, which facilitates the transfer of heat. In contrast, the temperature fluctuations in the NW are limited to 0–600 mm, with little change in the deeper parts of the wall throughout the day. Besides, the temperature level of the NCW was significantly higher than that of the NW at different depths.

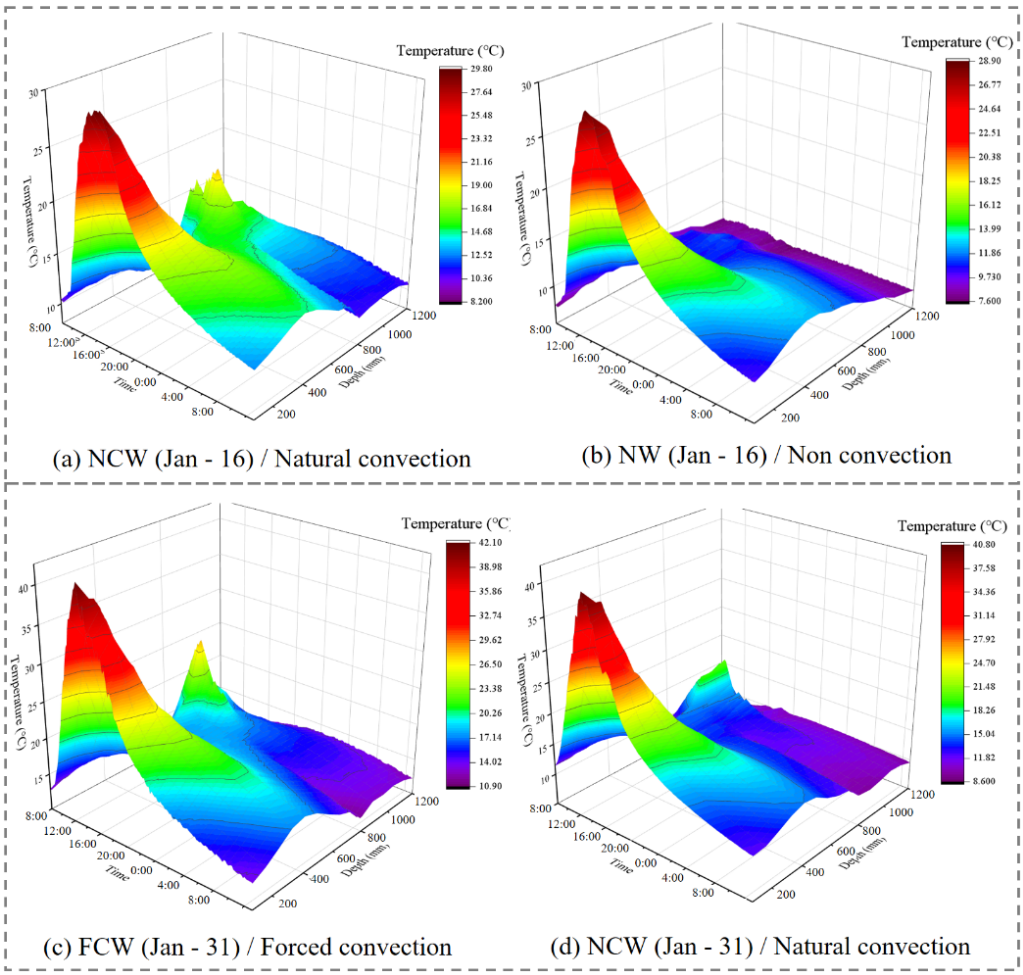

Figure 6. Internal temperature distribution of the wall with blocked internal convection (NW), wall with natural internal convection (NCW), and wall with forced internal convection (FCW) on a sunny day.

The temperature distribution of the NCW demonstrates that the air convection catalyzed an increase in the heat exchange between the cultivation space and the hollow layer and caused the deeper wall materials to engage in heat storage and release. The temperature distribution of the NW indicates that the heat storage depth of the wall was limited. The NW only delayed the temperature drop and had a thermal insulation effect [37].

Additionally, another day (31 January 2018) was chosen as the representative day for comparing the FCW and NCW (Figure 6c,d). The average nighttime temperature was −5.0 °C and the average daytime temperature was 3.4 °C. The highest outdoor temperature was 6.2 °C, and the lowest outdoor temperature was −10.3 °C. Both the NCW and FCW demonstrate temperature fluctuation in deep part, indicating that both natural convection and forced convection promote heat exchange between the hollow layer and cultivation space. However, the FCW had a better temperature level in contrast to the temperature distribution of the NCW. This is attributed to steady circulating airflow of forced convection without relying on thermal pressure.

After specifying the variation throughout the day, the focus is on comparing the temperature distribution at a typical time. First, 14:00 was chosen as the typical heat storage time, and 06:00 was chosen as the typical heat release time.

At the typical heat storage time, both the NCW and NW had the highest temperature at the wall surface in the inner layer (0–400 mm) (Figure 7a,b). Then, the NCW demonstrated a slower temperature decrease than NW, and it was 2.3 °C warmer than the NW at the depth with the lowest temperature (340 mm). However, the temperature of NCW had a rapid rebound and the temperature difference expanded to 4.3 °C at 400 mm. The circulating airflow as a low temperature heat source effectively improved the temperature distribution in the inner layer of the wall. In the outer layer, thanks to the hot air being introduced into the hollow layer, the temperature difference between NCW and NW at 1000 mm reached 4.8 °C, which is a good proof that the circulating airflow can drive the deep wall material to participate in the heat storage process. Additionally, judging from the temperature difference of up to 8.1 °C between the two hollow layers, the heat that can be brought into the interior of the wall with the circulating airflow is significant enough to have an impact on the temperature distribution of the deep material.

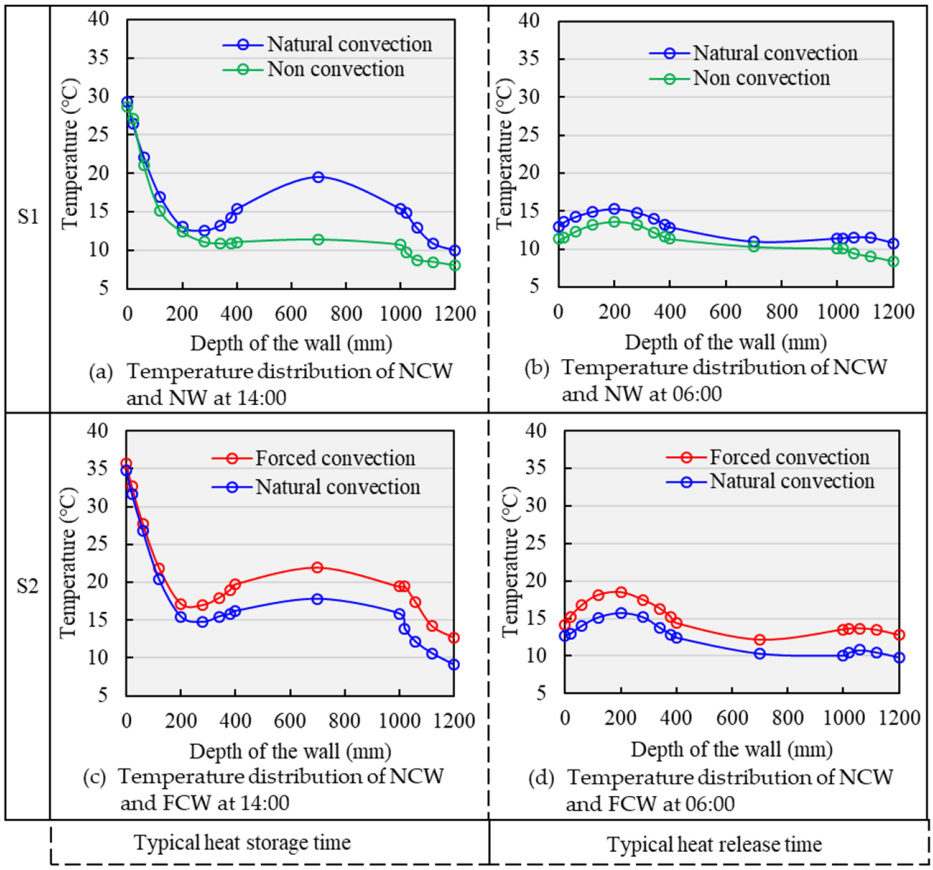

Figure 7. Temperature distribution in the wall at the typical thermal storage time (14:00) and release time (06:00) on a sunny day. Note: Wall depth was calculated in the indoor direction to the outdoor direction.

At the typical heat release time, the temperature level of the NCW was significantly higher than that of the NW, and the average temperature of the NCW was higher than that of the NW by 1.7 °C. Thus, natural convection enhanced the heat release capacity of the wall at night. In the hollow layer (400–1000 mm), the air temperatures of the NCW and NW were lower than those of the walls on both sides, indicating that there was a heat release from the wall surfaces to the air of hollow layer at night.

For the comparison of FCW and NCW (Figure 7c,d), the air temperature in the hollow layer of the FCW was 4.2 °C higher than that of the NCW, indicating that the temperature of the airflow introduced via forced convection was higher. The reason for this is that the generation of natural convection requires a temperature difference, leading to temperature lag. Forced convection produces a greater heat storage capacity effect. Besides, the wall temperature level of the FCW was higher at the typical heat release time than that of the NCW. Additionally, the air temperature of the FCW hollow layer was clearly lower than the wall temperature on both sides. This was due to a more thorough heat exchange due to forced convection.

3.3. Heat Flux on Different Surfaces of the North Wall

Negative heat flux indicates that heat flows from the north wall to the indoor environment (heat release) and positive heat flux indicates that heat flows from the indoor environment to the north wall (heat storage). The results of the north wall temperature distribution (Figure 6) indicated that there were three surfaces involved in heat storage and release in the north wall: the indoor surface, the hollow layer's south surface, and the hollow layer's north surface. Thus, the continuous heat flux changes of the three surfaces were monitored (Figure 8). The heat storage and release patterns of the hollow layer and the indoor surface were similar over seven consecutive days of observation, and there were evident heat absorption and release effects. The heat flux of the indoor surface was significantly greater than that of the other surfaces. During the day, the maximum heat flux of the NCW indoor surface reached 220.7 W m^{-2}, and at night, the heat flux reached 72.1 W m^{-2}. These results demonstrate that the north wall has an essential role in heat storage and release in CSGs. The two surfaces of the hollow layer also assisted in heat storage and release. During the day, the heat storage of the north surface was slightly higher than that of the south surface. The FCW demonstrated a more stable and efficient ability for heat storage, and the maximum heat flux was 67.3 W m^{-2} on the north surface. At night, the south surface heat flux was better than that of the north surface. The heat flux of the FCW and NCW reached 19.8 and 13.8 W m^{-2}, respectively. The outer wall was exposed to the outside environment, resulting in a large heat loss. The temperature difference between the air and the south surface was lower than the difference between the air and the north surface, therefore, the north surface absorbed more heat during the day and released less heat at night.

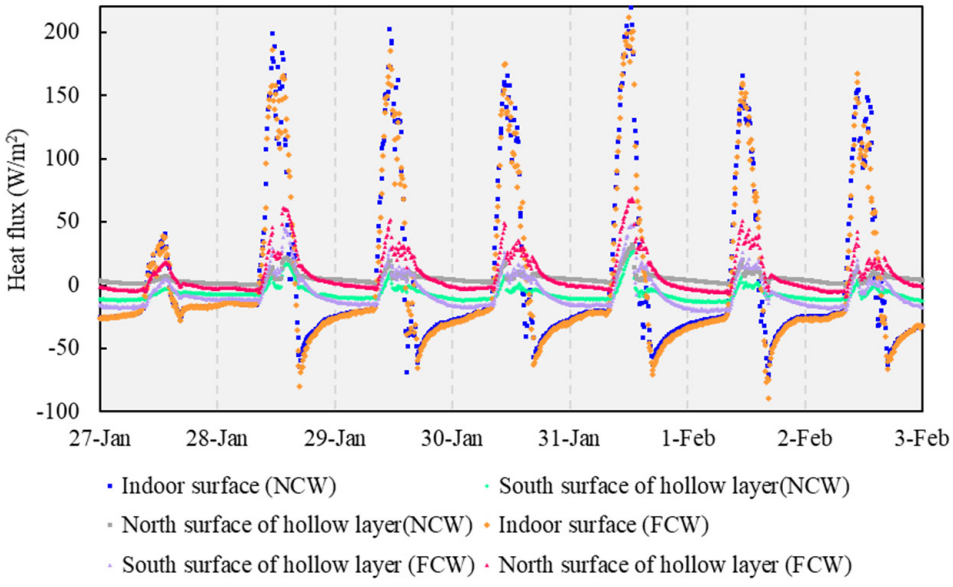

Figure 8. Heat flux of different surfaces of the NCW and FCW.

The ratios of heat storage and release of the three surfaces were calculated (Figure 9). The key heat storage and release portion was the indoor surface, contributing 77–84% (NCW) and 62–66% (FCW) of the heat storage as well as 73–76% (NCW) and 66–72% (FCW) of the heat release. For the NCW, the heat storage generated via natural convection accounted for 16–23%, and the heat release accounted for 25–28%. The results show that the heat storage of the north surface is higher and that the heat release of the south surface is higher. For the FCW, the heat storage and release generated via forced convection accounted for 34–38% and 28–34%, respectively. From the overall ratio, the heat storage and release effect of forced convection is better than that of natural convection.

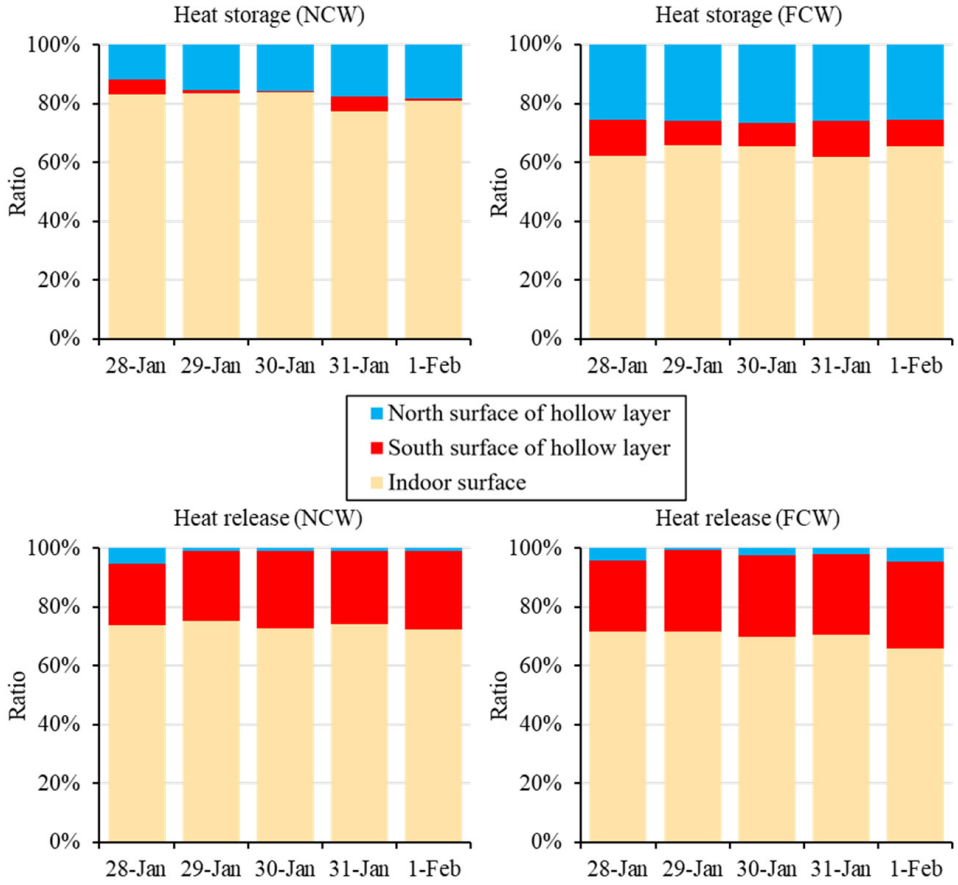

Figure 9. Ratio of heat storage and release of the different surfaces over several days.

The heat storage and release ratios of the north and south surfaces in both of the FCW and NCW were unequal. The north surface (belonging to the outer layer of the hollow wall) absorbed more heat during the day, but released less during the night. The reason is that the outer layer of the hollow wall is closer to the external environment in terms of location, and the continuous heat dissipation into the outdoors reduces the amount of heat that can be used for heating, resulting in a lower contribution to the indoor temperature. In comparison, the south surface of the hollow layer loses less heat, allowing more heat to be available for CSG's air heating. Therefore, the south surface of the hollow layer provided a lower ratio of heat storage and a larger ratio of heat release than the north surface. Increasing the thickness of the insulation layer on the basis of the current north wall design would improve the thermal performance of the outer layer of the hollow wall in extremely cold conditions.

Figure 10 shows the thermal images of the indoor surfaces of the FCW and the NCW at 06:00 when the outdoor temperature was −16.6 °C (24 January 2018). At 06:00, the temperature ranges of the indoor surfaces of the FCW and NCW were 7.6 °C–9.8 °C and 8.1 °C –9.7 °C, respectively. At this time, the wall remained in an exothermic heat state and

the upper and lower vents of the FCW had a large temperature difference. The temperature of the upper vents was lower than that of the lower vents because of the constant operation of the fans. Additionally, the temperature of the upper and lower vents was closer in the NCW, therefore, the natural convection effect at this time was weak.

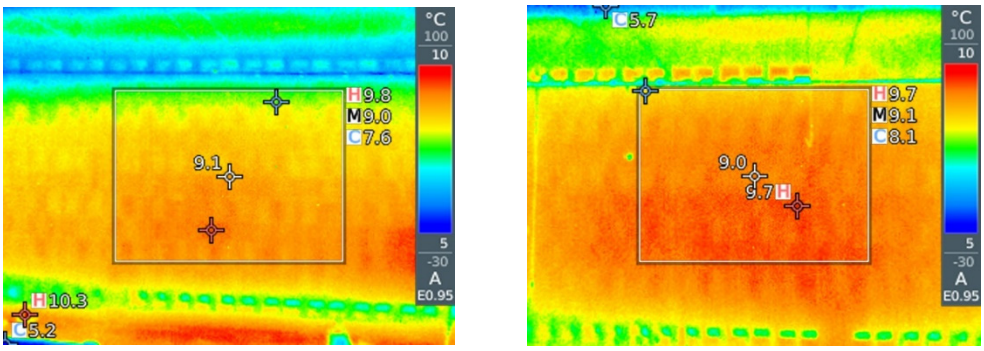

Figure 10. Wall surface temperatures of the FCW and NCW at 06:00 (January 24, 2018): (**a**) FCW; and (**b**) NCW.

3.4. Air Convection under Different Strategies

The basic condition for the formation of natural convection is a certain difference in temperature between the hollow layer and the space of cultivation, therefore, the velocity of air circulation and the temperature difference characterize the airflow pattern. The air velocity of the upper and lower vents of the NCW and the FCW revealed different trends during observation over several days (Figure 11).

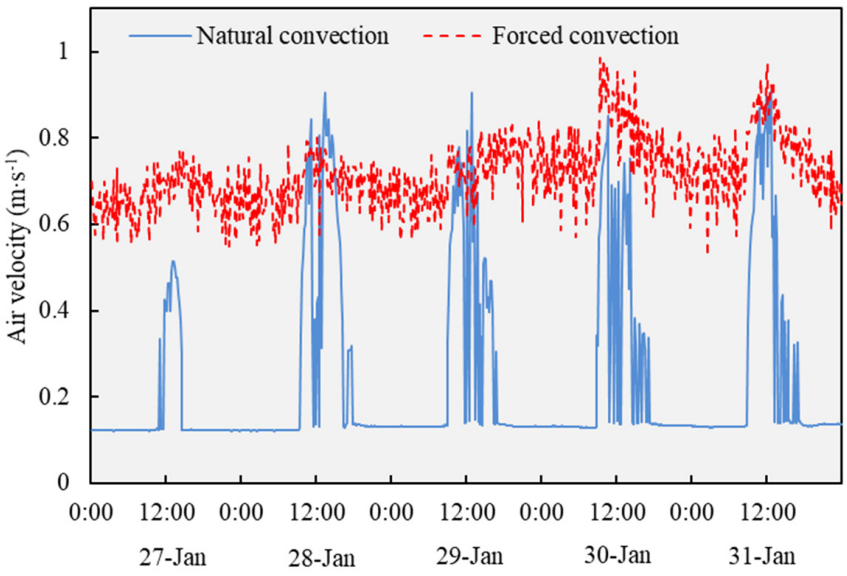

Figure 11. Air velocity of the vents under natural convection and forced convection.

Figure 11 shows the variations of air velocity for natural convection and forced convection during the observation period. The difference in air velocity between daytime and nighttime natural convection was large, with average air velocity ranging from 0.47 to 0.53 $m \cdot s^{-1}$ during the day on sunny days, but falling below 0.15 $m \cdot s^{-1}$ at night. The strongest natural convection occurred in the midday, and the air velocity was comparable to that of forced convection. On January 28 and 29, both of the maximum air velocities of the natural convection were 0.90 $m \cdot s^{-1}$, which were higher than the air velocity of the

forced convection. The results show that sufficient circulating airflow can be created for heat storage during the daytime by the air density difference.

The diurnal air velocity variation of forced convection was relatively small, remaining between the range of 0.55–0.95 $m \cdot s^{-1}$. The daytime air velocity of natural convection was weakened (0.39 $m \cdot s^{-1}$) by the reduced temperature difference between the hollow layer and the cultivated space on a cloudy day, but forced convection provided stronger airflow (0.70 $m \cdot s^{-1}$) which promoted heat storage on a cloudy day. Under unfavorable weather conditions, the stronger convective heat transfer effect of forced convection mobilized more accumulated heat in the wall which is of great significance for maintaining the thermal environment in CSGs.

Besides, the direction of airflow circulation can be optimized by fans. From the perspective of benefiting the crop growth, it is necessary to configure double-direction fans for reversing the direction of natural convection that forcing the cooled air into the CSG from the upper vents during the day and forcing the warm air into the CSG from the lower vents at night.

Figure 12 shows the temperature differences between the upper and lower vents of the NCW and the FCW from 27 to 31 January 2018. 27 January was a typical cloudy day. The temperature differences between the upper and lower vents of the NCW and the FCW were higher during the day and lower at night, and the peak in temperature differences occurred at noon whether it was a sunny or a cloudy day. This trend is closely connected to the solar radiation obtained by the CSG.

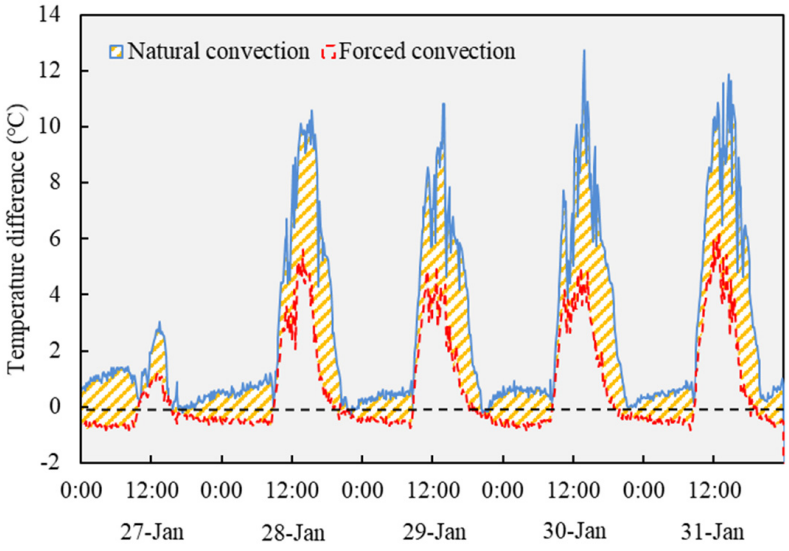

Figure 12. Temperature difference between the upper and lower vents of the NCW and FCW.

For the NCW, the temperature difference changed dramatically as the solar radiation increased during the day, and the mean temperature difference at noon exceeded 12 °C. Thus, the wall structure had the requisite conditions for air convection during operation. The temperature difference at night was lower, resulting in weak air velocity, but the hollow layer still played the role of heating the air according to the night temperature distribution and heat flux of the wall (Figures 6 and 8).

The change pattern of the FCW was similar to that of the NCW, but there was a slightly smaller average temperature difference. During the day, the maximum difference in temperature was only 6.2 °C. The lower temperature difference demonstrates that air exchange in the hollow layer is faster because of the fans, allowing a more efficient heat transfer between the hollow layer and the cultivation space.

The temperature difference between the upper and lower vents varies with the environmental temperature. When the temperature difference is zero, it means that the circulating airflow stagnates and enters the flipping period, following which the circulating airflow

of natural convection is gradually enhanced in the opposite direction as the temperature difference increases again. The air circulation directions of natural convection and forced convection at night are the same, and the role of forced airflow is to promote the exchange of heat at night. However, the temperature difference between the upper and lower vents of the NCW was positive, whereas the difference of the FCW was negative. The high air velocity generated by the fans creates a "local low temperature zone" near the upper vents, resulting in a negative temperature difference between upper and lower vents.

3.5. Heat Transfer Capacity of the Air Convection in the Hollow Layer

Natural convection heat transfer is a typical thermal pressure ventilation process, and the airflow can be calculated on the basis of the temperature of the upper and lower vents. Forced convection is constant because of the strong airflow, and the measured air velocity is used to calculate the airflow. The convective heat exchange process of the circulating airflow includes changes in sensible heat and latent heat. The change in latent heat produced by the condensation of water vapor in the hollow layer is not negligible. Thus, the heat exchange of the air convection in the hollow layer is calculated using the air state of the upper and lower vents. In this section, the airflow and heat transfer through the upper vents are calculated based on a 60 m north wall in a CSG and the results are shown in Figure 13.

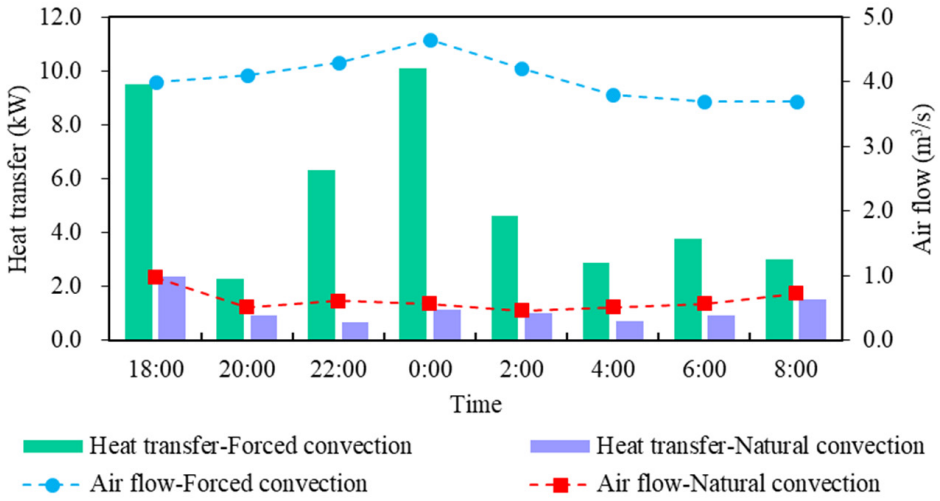

Figure 13. Airflow and heat transfer of forced and natural convection at night (January 23).

During the day, both natural and forced convections generated good air circulation, and the convection heat transfer became stronger. To calculate the airflow and heat transfer of air convection, 14:00 was chosen as the typical heat storage time. At 14:00, the airflow of natural convection and forced convection were 2.62 and 4.29 $m^3 \cdot s^{-1}$, respectively. At 14:00, the temperature difference between the hollow layer and the cultivation space was the greatest and the convection heat exchange was the highest, both of which resulted in the best heat exchange performance. The efficient airflow brought extensive heat exchange. The maximum heat transfers of natural convection and forced convection during the day were 31.5 and 52.2 kW, respectively. Forced convection maintained an uninterrupted and strong air circulation because of the fans, and the airflow and temperature levels of the hollow layer were better than those in natural convection.

Natural convection is weak at night because of the small temperature difference. However, the changes in heat exchange in the hollow layer of the two convection strategies at night must be confirmed, so the airflow and heat exchange throughout the night were calculated (Figure 13). The airflow of natural convection at night was maintained at a low level of 0.5–0.6 $m^3\ s^{-1}$ from 20:00 to 06:00 (the next day). Forced convection was maintained at a high flow level. After 20:00, airflow rose slightly and reached a maximum value of 4.7 $m^3\ s^{-1}$ at 00:00. Afterward, it showed a downward trend. The large airflow

difference between the two strategies led to the difference in heat transfer capacity. The forced convection heat transfer change trend was similar to the change in the airflow trend. The heat transfer capacity of air convection rose continuously from 20:00 to 00:00 and achieved a maximum value of 10.1 kW. This result indicates that the hollow structure had a high heat exchange potential when using the forced convection strategy. The heat release slowed down after midnight and fluctuated in the range of 2.9–4.6 kW. The heat transfer of natural convection at night is significantly lower than that of forced convection, fluctuating between 0.7 and 2.4 kW. The results indicate that forced convection creates a relatively more fluctuating heat transfer and higher heat release than natural convection, which facilitates the full release of the stored heat in the hollow layer. Therefore, forced convection can compensate for natural convection, which is limited by the air density difference at night and made the heat release more sufficient.

3.6. Dehumidification Potential of Hollow Layer

The convective heat exchange process of the circulating airflow in the hollow layer contains both sensible heat and latent heat changes. The latent heat change is mainly the process of condensation of hot air after entering the hollow layer. Thus, the wall structure has a certain dehumidification potential. During the experiment, a large amount of condensed water was observed in the hollow layer, especially at noon when the convection heat exchange was strong. However, there was no water collection tank to collect the condensate in the current wall design scheme, even if it is possible to dehumidify during the day, this moisture will be brought back into the CSG at night. Therefore, the dehumidification potential is calculated to provide an evidence for improving the wall design. It should be noted that the experiment was in a CSG without any plants, which modify seriously the heat and water vapor balances. Theoretically, the dehumidification potential of an empty CSG can be estimated by the humidity change of the air flowing through the upper and lower vents and the airflow rate. When the natural convection was strongest at 14:00, the circulating air of the entire north wall removed 4.8 g of water vapor per second, meaning that the maximum instantaneous dehumidification capacity of the entire CSG (480 m^2) reached 17.3 $kg{\cdot}h^{-1}$. The 4.8 g of water vapor per second means 11 kW of latent heat and compared with the 31.5 kw of natural convection heat transfer at noon, the ratio of latent heat to sensible heat is 0.53. Therefore, when the convection heat exchange was strong, the wall structure had a certain dehumidification potential, which had a positive effect on the regulation of the humid environment in the CSGs. The condition for exercising the dehumidification capacity of the wall is to configure condensate collection tank on the existing design to remove excess water vapor from the hollow layer and prevent condensed water to be re-evaporated from the wall during the night.

3.7. Accumulated Heat and COP

Figure 14 shows the comparison of the FCW and the NCW daily accumulated heat storage and release results for 5 days. The results indicate that both strategies produced strong heat storage and release results under sunny conditions, and the FCW was superior to the NCW in terms of heat storage and release. There was a large difference between the heat storage of the two strategies. The total heat storage of the FCW and the NCW was 3.8 and 3.0 $MJ{\cdot}m^{-2}{\cdot}d^{-1}$, respectively. The heat storage of the FCW was 25.7% higher. The FCW and the NCW had an average heat release of 2.7 and 2.4 $MJ{\cdot}m^{-2}{\cdot}d^{-1}$, respectively, and the heat release of the FCW was 10.7% more than the NCW. Natural convection clearly enhanced the heat storage and release potential of the wall, and this effect was further improved via forced convection. Hence, a mixed working strategy of natural and forced convections can be appropriately adopted to obtain economical and effective heat exchange effects.

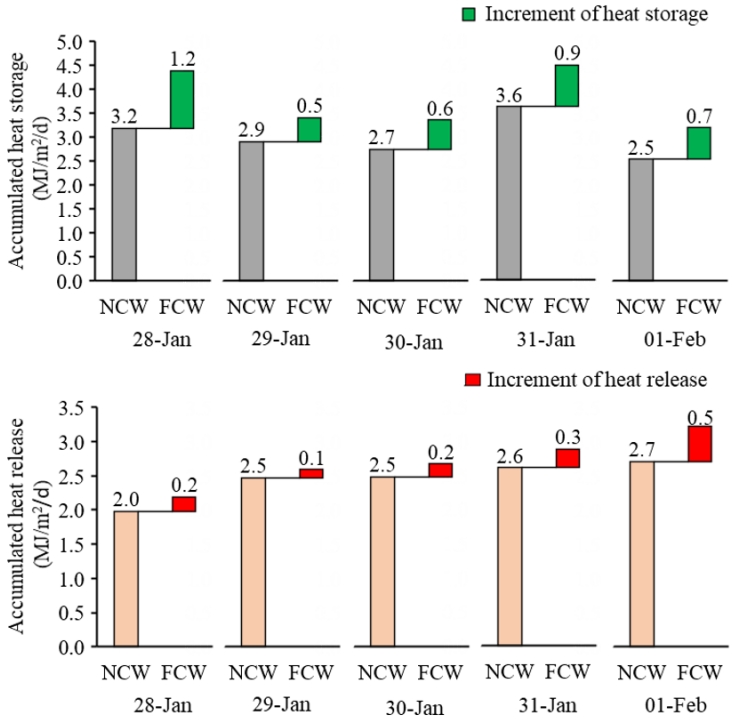

Figure 14. Daily accumulated heat storage and release of the NCW and FCW.

For forced convection, the power of fans was 3.6 $W \cdot m^{-2}$ and the energy consumption of fans was 0.3 $MJ \cdot m^{-2} \cdot d^{-1}$. Taking the hollow layer with the fans as an active solar heating system, the COP floats in the range of 1.9 to 3.4, which is a relatively efficient performance compared with some other types of heating systems, such as water source heat pumps (2.9–7.0) [38–40], soil source heat pumps (3.8) [41] and air source heat pumps (2.7) [42]. However, it should be noted that the circulating airflow actually only provides no more than 20 °C of hot air at night, far less than other heat pump systems, while the benefit is the lower energy consumption.

In this study, the fans' runtime has an impact on the COP. The results of air velocity and heat flux proved that natural convection has a strong heat storage capacity during the daytime. Therefore, a combination of natural convection and forced convection should be used to improve the COP by adjusting the fans' runtime, which is beneficial for reducing energy consumption.

4. Conclusions

The north wall is the key structure to maintain the thermal environment in the Chinese solar greenhouse, and the design and renovation of the north wall has long been a hot topic. In order to expand the heat transfer surface and increase the heat storage volume of the north wall in CSGs, this study proposed a design of air convection north wall with a hollow layer for CSGs. Additionally, field tests were conducted to compare the different convection strategies via temperature, airflow and heat transfer efficiency. The results from this study have indicated that:

(1) The design of air convection north wall with a hollow layer improves the indoor thermal environment at night. The differences between indoor and outdoor air temperatures of NCW and NW at night were 17.3 °C and 16.0 °C, respectively, and the differences of the NCW and FCW at night were 17.2 °C and 18.2 °C, respectively. The north wall keeps the CSG well above 5 °C despite outdoor temperatures of −16.3 °C during the night.

(2) The circulating air flow significantly improves the internal temperature distribution in the north wall, indicating more wall materials participate in the heat storage and heat release process.
(3) Air circulated through the hollow wall contributes significantly to the heat exchange between north wall and CSG. When generated by natural convection heat storage and release accounted for 16–23% and 25–28%, while the heat storage and release generated via forced convection accounted for 34–38% and 28–34%.
(4) Given the additional heating power provided by the hollow layer of the north wall during the night (on average 1.2 kW by natural convection and 5.3 kW by forced convection), the north wall plays an important role in maintaining a favorable temperature inside a CSG.
(5) The COP of the active solar heating system (a hollow layer with the fans) ranged from 1.9 to 3.4. Although the COP is relatively efficient, the circulating airflow only provides no more than 20 °C of hot air at night, far less than other heat pump systems, while the benefit is the low energy consumption.
(6) Compared with natural convection, forced convection has advantages in airflow controllability, heat exchange efficiency and heat accumulation. However, natural convection has a strong heat transfer capacity at noon. Therefore, the combination of the two convection strategies can get a good effect.
(7) This study was performed in a crop-less CSG, and the thermal and water-vapor transfers were different from a CSG with crops inside. Therefore, it is necessary to carry out the next experiment to explore the moisture and heat balance in the CSG under the influence of crops and fully evaluate the impacts of the north wall on the comfort of the indoor environment.

Author Contributions: Conceptualization, Y.Z., S.Z., J.C. and C.M.; methodology, Y.Z. and C.M.; formal analysis, Y.Z., S.Z., P.W., N.L., W.X., K.Z. and C.M.; Study design, J.C.; investigation, Y.Z. and K.Z.; resources, S.Z. and W.X.; writing—original draft preparation, Y.Z. and K.Z.; writing—review and editing, S.Z., J.C., P.W., C.M., W.X. and N.L.; supervision, S.Z.; project administration, J.C. and P.W.; funding acquisition, S.Z. All authors have read and agreed to the published version of the manuscript.

Funding: This research was funded by the National Key R&D Program of China, grant number 2019YFD1001900 and China Agriculture Research System of MOF and MARA, grant number CARS-23-D02.

Institutional Review Board Statement: Not applicable.

Informed Consent Statement: Not applicable.

Data Availability Statement: Not applicable.

Conflicts of Interest: The authors declare no conflict of interest.

References

1. Cao, K.; Xu, H.; Zhang, R.; Xu, D.; Yan, L.; Sun, Y.; Xia, L.; Zhao, J.; Zou, Z.; Bao, E. Renewable and sustainable strategies for improving the thermal environment of Chinese solar greenhouses. *Energy Build.* **2019**, *202*, 109414. [CrossRef]
2. Kendirli, B. Structural analysis of greenhouses: A case study in Turkey. *Build. Environ.* **2006**, *41*, 864–871. [CrossRef]
3. Panwar, N.L.; Kaushik, S.C.; Kothari, S. Solar greenhouse an option for renewable and sustainable farming. *Renew. Sustain. Energy Rev.* **2011**, *15*, 3934–3945. [CrossRef]
4. Gao, L.H.; Qu, M.; Ren, H.Z.; Sui, X.L.; Chen, Q.Y.; Zhang, Z.X. Structure, function, application, and ecological benefit of a single-slope, energy-efficient solar greenhouse in China. *Horttechnology* **2010**, *20*, 626–631. [CrossRef]
5. Li, A.; Huang, L.; Zhang, T. Field test and analysis of microclimate in naturally ventilated single-sloped greenhouses. *Energy Build.* **2017**, *138*, 479–489. [CrossRef]
6. Tong, G.; Christopher, D.M.; Li, T.; Wang, T. Passive solar energy utilization: A review of cross-section building parameter selection for Chinese solar greenhouses. *Renew. Sustain. Energy Rev.* **2013**, *26*, 540–548. [CrossRef]
7. Ghasemi Mobtaker, H.; Ajabshirchi, Y.; Ranjbar, S.F.; Matloobi, M. Solar energy conservation in greenhouse: Thermal analysis and experimental validation. *Renew. Energy* **2016**, *96*, 509–519. [CrossRef]

8. Beshada, E.; Zhang, Q.; Boris, R. Winter performance of a solar energy greenhouse in southern Manitoba. *Can. Biosyst. Eng./ Le Genie Des. Biosyst. Can.* **2006**, *48*, 1–8.
9. Liu, X.; Wu, X.; Xia, T.; Fan, Z.; Shi, W.; Li, Y.; Li, T. New insights of designing thermal insulation and heat storage of Chinese solar greenhouse in high latitudes and cold regions. *Energy* **2022**, *242*, 122953. [CrossRef]
10. Liu, H.; Yin, C.; Hu, X.; Tanny, J.; Tang, X. Microclimate characteristics and evapotranspiration estimates of cucumber plants in a newly developed sunken solar greenhouse. *Water* **2020**, *12*, 2275. [CrossRef]
11. Hou, Y.; Li, A.; Li, Y.; Jin, D.; Tian, Y.; Zhang, D.; Wu, D.; Zhang, L.; Lei, W. Analysis of microclimate characteristics in solar greenhouses under natural ventilation. *Build. Simul.* **2021**, *14*, 1811–1821. [CrossRef]
12. Akrami, M.; Salah, A.H.; Javadi, A.A.; Fath, H.E.S.; Hassanein, M.J.; Farmani, R.; Dibaj, M.; Negm, A. Towards a sustainable greenhouse: Review of trends and emerging practices in analysing greenhouse ventilation requirements to sustain maximum agricultural yield. *Sustainability* **2020**, *12*, 2794. [CrossRef]
13. Iddio, E.; Wang, L.; Thomas, Y.; McMorrow, G.; Denzer, A. Energy efficient operation and modeling for greenhouses: A literature review. *Renew. Sustain. Energy Rev.* **2020**, *117*, 109480. [CrossRef]
14. Chen, W.; Liu, W. Numerical and experimental analysis of convection heat transfer in passive solar heating room with greenhouse and heat storage. *Sol. Energy* **2004**, *76*, 623–633. [CrossRef]
15. Zhang, L.; Xu, P.; Mao, J.; Tang, X.; Li, Z.; Shi, J. A low cost seasonal solar soil heat storage system for greenhouse heating: Design and pilot study. *Appl. Energy* **2015**, *156*, 213–222. [CrossRef]
16. Sethi, V.P.; Sumathy, K.; Lee, C.; Pal, D.S. Thermal modeling aspects of solar greenhouse microclimate control: A review on heating technologies. *Sol. Energy* **2013**, *96*, 56–82. [CrossRef]
17. Qing-yun, C. Progress of practice and theory in sunlight greenhouse. *J. Shanghai Jiaotong Univ. (Agric. Sci.)* **2008**, *5*, 343–350.
18. Bastien, D.; Athienitis, A.K. Passive thermal energy storage, part 1: Design concepts and metrics. *Renew. Energy* **2018**, *115*, 1319–1327. [CrossRef]
19. Wang, J.; Li, S.; Guo, S.; Ma, C.; Wang, J.; Sun, J. Analysis of heat transfer properties of hollow block wall filled by different materials in solar greenhouse. *Eng. Agric. Environ. Food* **2017**, *10*, 31–38. [CrossRef]
20. Zhang, G.; Shi, Y.; Liu, H.; Fei, Z.; Liu, X.; Wei, M.; Liu, F.; Wang, S. Heat transfer performance of an assembled multilayer wall in a Chinese solar greenhouse considering humidity. *J. Energy Storage* **2021**, *33*, 102046. [CrossRef]
21. Ren, J.; Zhao, Z.; Zhang, J.; Wang, J.; Guo, S.; Sun, J. Study on the hygrothermal properties of a Chinese solar greenhouse with a straw block north wall. *Energy Build.* **2019**, *193*, 127–138. [CrossRef]
22. Zhang, X.; Lv, J.; Dawuda, M.M.; Xie, J.; Yu, J.; Gan, Y.; Zhang, J.; Tang, Z.; Li, J. Innovative passive heat-storage walls improve thermal performance and energy efficiency in Chinese solar greenhouses for non-arable lands. *Sol. Energy* **2019**, *190*, 561–575. [CrossRef]
23. Berroug, F.; Lakhal, E.K.; El Omari, M.; Faraji, M.; El Qarnia, H. Thermal performance of a greenhouse with a phase change material north wall. *Energy Build.* **2011**, *43*, 3027–3035. [CrossRef]
24. Boulard, T.; Razafinjohany, E.; Baille, A.; Jaffrin, A.; Fabre, B. Performance of a greenhouse heating system with a phase change material. *Agric. For. Meteorol.* **1990**, *52*, 303–318. [CrossRef]
25. Wang, H.; Li, X.; Zou, Z. Application of brick wall with phase change rice husk in solar greenhouse. *Trans. Chin. Soc. Agric. Eng.* **2011**, *27*, 253–257.
26. Guan, Y.; Chen, C.; Li, Z.; Han, Y.; Ling, H. Improving thermal environment in solar greenhouse with phase-change thermal storage wall. *Trans. Chin. Soc. Agric. Eng.* **2012**, *28*, 194–201.
27. Guan, Y.; Chen, C.; Ling, H.; Han, Y.; Yan, Q. Analysis of heat transfer properties of three-layer wall with phase-change heat storage in solar greenhouse. *Trans. Chin. Soc. Agric. Eng.* **2013**, *29*, 166–173.
28. Li, Y.; Yue, X.; Zhao, L.; Xu, H.; Liu, X.; Li, T. Effect of north wall internal surface structure on heat storage-release performance and thermal environment of Chinese solar greenhouse. *J. Build. Phys.* **2021**, *45*, 507–527. [CrossRef]
29. Yang, J.; Zou, Z.; Zhang, Z.; Wang, Y.; Zhang, Z.; Yan, F. Optimization of earth wall thickness and thermal insulation property of solar greenhouse in Northwest China. *Trans. Chin. Soc. Agric. Eng.* **2009**, *25*, 180–185.
30. Peng, D.; Zhang, Y.; Fang, H.; Yang, Q.; Wei, L. MATLAB simulation of one-dimensional heat transfer and heat flux analysis of north wall in Chinese solar greenhouse. *J. China Agric. Univ.* **2014**, *19*, 174–179.
31. Zhao, S.; Zhuang, Y.; Zheng, K.; Ma, C.; Cheng, J.; Ma, C.; Chen, X.; Zhang, T. Thermal performance experiment on air convection heat storage wall with cavity in Chinese solar greenhouse. *Trans. Chin. Soc. Agric. Eng.* **2018**, *34*, 223–231.
32. Xu, W.; Song, W.; Ma, C. Performance of a water-circulating solar heat collection and release system for greenhouse heating using an indoor collector constructed of hollow polycarbonate sheets. *J. Clean. Prod.* **2020**, *253*, 119918. [CrossRef]
33. Sun, Y. *Concise Ventilation Design Manual*; China Architecture Building Press: Beijing, China, 1997.
34. Ma, C. *Agricultural Bioenvironmental Engineering*; China Architecture Building Press: Beijing, China, 2006.
35. Yang, S.; Tao, W. *Heat Transfer*, 4th ed.; China Higher Education Press: Beijing, China, 2006.
36. Lu, W.; Zhang, Y.; Fang, H.; Ke, X.; Yang, Q. Modelling and experimental verification of the thermal performance of an active solar heat storage-release system in a Chinese solar greenhouse. *Biosyst. Eng.* **2017**, *160*, 12–24. [CrossRef]
37. Xiaodan, Z.; Jianming, X.; Jihua, Y.; Jian, L. Simulation analysis of thermal properties of air enclosure covered with aluminum foil in wall of solar greenhouse. *Trans. Chin. Soc. Agric. Eng.* **2017**, *2*, 227–233.

38. Ming, L.; Han, L.; Weitang, S. Application of active heat system developed with capillary tube mates in Chinese solar greenhouse. *Trans. Chin. Soc. Agric. Mach.* **2019**, *50*, 341–349.
39. Ke, X.; Yang, Q.; Zhang, Y.; Fang, H.; He, Y.; Zhang, C. Warming effect comparison between substrate warming system and air warming system by active heat storage-release in Chinese solar greenhouse. *Trans. Chin. Soc. Agric. Eng.* **2017**, *33*, 224–232.
40. Fang, H.; Yang, Q.; Zhang, Y.; Sun, W.; Lu, W.; Liang, H. Performance of a solar heat collection and release system for improving night temperature in a Chinese solar greenhouse. *Appl. Eng. Agric.* **2015**, *31*, 283–289.
41. Chai, L.; Ma, C.; Ni, J.-Q. Performance evaluation of ground source heat pump system for greenhouse heating in northern China. *Biosyst. Eng.* **2012**, *111*, 107–117. [CrossRef]
42. Sun, W.; Guo, W.; Xu, F.; Wang, L.; Xue, X.; Li, Y.; Chen, Y. Application effect of surplus air heat pump heating system in Chinese solar greenhouse. *Trans. Chin. Soc. Agric. Eng.* **2015**, *31*, 235–243.